HHS Public Access

Author manuscript

Nat Immunol. Author manuscript; available in PMC 2014 February 01.

Published in final edited form as:

Nat Immunol. 2013 August ; 14(8): 831–839. doi:10.1038/ni.2622.

The Nuclear Receptor LXRα controls the functional specialization of splenic macrophages

Noelia A-Gonzalez[1,2,3,11], **Jose A. Guillen**[1,2,11], **Germán Gallardo**[2,11], **Mercedes Diaz**[1,2,11], **Juan V. de la Rosa**[2], **Irene H. Hernandez**[1,2], **Maria Casanova-Acebes**[3], **Felix Lopez**[2], **Carlos Tabraue**[2], **Susana Beceiro**[1,2], **Cynthia Hong**[4], **Pedro C. Lara**[5], **Miguel Andujar**[6], **Satoko Arai**[7], **Toru Miyazaki**[7], **Senlin Li**[8,9], **Angel L. Corbi**[10], **Peter Tontonoz**[4], **Andres Hidalgo**[3], and **Antonio Castrillo**[1,2]

[1]Instituto de Investigaciones Biomédicas “Alberto Sols” CSIC-Universidad Autonóma de Madrid, Spain

[2]Unidad Asociada de Biomedicina IIBM CSIC-Universidad de Las Palmas de Gran Canaria, Las Palmas Spain

[3]Department of Epidemiology, Atherothrombosis and Imaging, Centro Nacional de Investigaciones Cardiovasculares, CNIC Madrid, Spain

[4]Howard Hughes Medical Institute, Department of Pathology and Laboratory Medicine, University of California Los Angeles, California USA

[5]Servicio de Oncología Radioterápica, Hospital Universitario de Gran Canaria Dr. Negrín, Las Palmas, Spain

[6]Servicio de Patología, Hospital Universitario Materno-Infantil de Las Palmas, Spain

[7]Laboratory of Molecular Biomedicine for Pathogenesis, Center for Disease Biology and Integrative Medicine, Faculty of Medicine, University of Tokyo, Japan

[8]Departments of Medicine and Pharmacology, University of Texas Health Science Center

[9]South Texas Veterans Health Care System, San Antonio, Texas, USA

[10]Centro de Investigaciones Biológicas, Consejo Superior de Investigaciones Científicas, Madrid, Spain

Correspondence should be addressed to A.C. (acastrillo@iib.uam.es), Antonio Castrillo, Ph.D., Instituto de Investigaciones Biomédicas “Alberto Sols”, Consejo Superior de Investigaciones Científicas-Universidad Autónoma de Madrid. Madrid, Spain and Unidad Asociada de Biomedicina Instituto de Investigaciones Biomédicas “Alberto Sols” IIBM CSIC-Universidad de Las Palmas de Gran Canaria, Spain, acastrillo@iib.uam.es.

[11]These authors contributed equally to this work

Author contributions

NA-G, JAG, GG and MD designed and perfomed experiments and analized data. JVDLR, IHH, MC-A, FL, CT and SB performed experiments. CH, PCL, MA, SA, TM, SL, ALC, PT and AH provided key reagents, intellectual input and analized or interpreted data. NA-G and AH also contributed to the writing of the manuscript. AC supervised the project, designed and performed experiments, analized data and wrote the manuscript.

Competing financial interests

The authors declare no competing financial interests

Abstract

Macrophages are professional phagocytic cells that orchestrate innate immune responses and display remarkable phenotypic diversity at different anatomical locations. However, the mechanisms that control the heterogeneity of tissue macrophages are not well characterized. Here, we report that the nuclear receptor LXRα is essential for the differentiation of macrophages in the marginal zone (MZ) of the spleen. LXR deficient mice are defective in the generation of MZ and metallophilic macrophages, resulting in abnormal responses to blood-borne antigens. Myeloid specific expression of LXRα or adoptive transfer of wild-type monocytes rescues the MZ microenvironment in LXRα deficient mice. These results demonstrate that LXRα signaling in myeloid cells is crucial for the generation of splenic MZ macrophages and reveal an unprecedented role for a nuclear receptor in the generation of specialized macrophage subsets.

Introduction

Macrophages have long been recognized as key components of cellular immunity. As sentinels of the immune system distributed throughout the body, macrophages ensure tissue integrity by scavenging altered host components, foreign materials and organisms[1]. Macrophages direct anti-microbial actions through the production of cytotoxic species, cytokines and chemokines that are required for the initiation and persistence of acute and chronic inflammation[2]. Macrophages, also contribute to immune suppression and self tolerance by removing apoptotic cells under non-inflammatory conditions[3].

Tissue macrophages were traditionally categorized as part of the mononuclear phagocyte system and have been generally considered to be derived from circulating monocytes or myeloid progenitor cells[4]. Monocytes and resident macrophages are largely dependent on macrophage colony-stimulating factor (CSF-1) and its receptor CSF-1R (also called CD115 or c-fms) for their differentiation and/or survival[1]. Tissue macrophages display a high degree of heterogeneity, a feature that reflects the individual functions of specialized macrophage populations at different anatomical locations[4, 5]. Functional diversity of macrophage populations is presumably determined by local signals present only under specific developmental, homeostatic or pathological tissue scenarios[4–6]. However, the molecular programs that control macrophage specialization and function in different tissues remain poorly defined.

The spleen is the largest secondary lymphoid organ in the body and is important for the generation of immune responses to blood-borne antigens and for filtering the blood of senescent cells or potentially noxious material[7]. These functions are linked to the phagocytic capacity of specific macrophage subpopulations that are compartimentalized into different splenic domains, including the red pulp (RP), the marginal zone (MZ) and the white pulp (WP)[1, 7, 8]. RP macrophages, defined by the expression of F4/80 and CD68 antigens, are critical for the phagocytosis of effete red blood cells and contribute to iron recycling[9]. In contrast, tingible body macrophages in the WP of the spleen express less F4/80 but express abundant CD68 and MFG-E8 and are involved in the engulfment of apoptotic lymphocytes generated during germinal center immune reactions[9]. The MZ is located at the interface of the WP and the RP where most of the arterial blood that enters the spleen can be screened by

several resident cell types, including two subsets of macrophages and a population of MZ B cells[8, 10]. Macrophages in this area form two concentric rings and present a special combination of surface receptors: MZ macrophages are characterized by the expression of SIGN-R1 and MARCO, whereas metallophilic macrophages express CD169. Based on their strategic position and their unique expression of pattern recognition receptors, MZ macrophages are believed to participate in many aspects of host immunity[8, 9]. The molecular and transcriptional regulators responsible for the generation of MZ macrophages remain undefined.

The Liver X receptors (LXRα, encoded by the gene *Nr1h3*, and LXRβ, encoded by the gene *Nr1h2*) are members of the nuclear receptor superfamily of transcription factors that play key roles in the control of sterol homeostasis[11]. LXRβ is expressed ubiquitously and LXRα is highly expressed in the liver, adipose tissue, intestine, and differentiated macrophages[11, 12]. In macrophages, where both LXRα and LXRβ are highly expressed, the two receptors transactivate a similar gene program, with the exception of the LXRα-specific target, *Cd5l*[12]. LXRs also regulate gene expression through a process known as transrepression[13, 14] and are important for the transcriptional responses of macrophages during engulfment of apoptotic cells[15]. Loss of LXRα and LXRβ in mice results in peripheral lipid accumulation and symptoms of immune overreaction that aggravate with age, culminating in systemic autoimmunity[15–17]. Since both LXRs activate and repress similar genetic programs in macrophages, it has been assumed that their functions in macrophages are largely redundant. Here, we demonstrate that expression of LXRα, but not LXRβ, in myeloid cells is crucial for the development of macrophages in the marginal zone of the spleen. Our results outline an unexpected role for a nuclear receptor in the genesis of tissue macrophage diversity.

Results

Absence of Marginal-Zone macrophages in LXR-deficient mice

To investigate a possible role of LXRs in the development of resident macrophages, tissue sections from wild-type and *Nr1h3*$^{-/-}$ *Nr1h2*$^{-/-}$ mice (lacking both LXRα and LXRβ, hereafter LXR-DKO) were screened by immunohistochemical analysis with monoclonal antibodies that recognize macrophage surface antigens[1]. Expression of F4/80 and CD68 markers was similar in wild-type and LXR-DKO tissues (Supplementary Fig. 1). Surprisingly, we found a complete absence of CD169+ macrophages in the spleens of LXR-DKO mice (Supplementary Fig. 1). In contrast, macrophages with CD169 expression were detected in several other tissues of LXR-DKO mice, such as lymph nodes, Peyer's patches, liver or intestine (Supplementary Fig. 1 and 2a). To further evaluate the impact of LXR expression on the development of the splenic macrophage repertoire, we used a combination of flow cytometry, immunofluorescence and immunohistochemical approaches. Expression of surface markers F4/80+, CD11b+ and CD68+ and the microanatomical location of these cells were comparable between wild-type and LXR-DKO spleens, suggesting that LXR signaling was not involved in the development of RP and WP macrophages under steady-state conditions (Fig. 1a, b). However, the distinctive microenvironment of the splenic MZ

was remarkably altered in LXR-DKO spleens (Fig. 1a, c). Indeed, expression of CD169, MARCO, SIGN-R1 and Tim-4 was selectively lost in LXR-DKO spleens (Fig. 1a–c).

Dysregulation of these phagocytic markers could reflect that their expression might be transcriptionally controlled by LXR signaling or that the cells expressing these proteins could be absent in LXR-DKO spleens. Expression of mRNA encoding MARCO, SIGN-R1 and CD169 was similar in LXR-DKO peritoneal macrophages compared to wild-type controls (Fig. 2a). In addition, the MZ space between the RP (containing cells positive for F4/80 or VCAM-1) and the border of the WP (delineated by MadCAM-1+ cells[18]), was virtually absent in LXR-DKO spleens (Fig. 2b). Hematoxilin and eosin staining and transmission electron microscopy further supported our finding that LXR signaling was crucial for the establishment of macrophages in the splenic MZ (Fig. 2b). Subpopulations of splenic dendritic cells (DCs) such as follicular DCs detected by FDC-M1, FDC-M2 markers[19] or Treml4+ cells[20] were also not different between wild-type and LXR-DKO spleens (Supplementary Fig. 2b).

Loss of MZ macrophages in LXR-DKO mice could be attributed to a defect in the local microenvironment (stromal non-hematopoietic network) or to deficient differentiation of hematopoietic precursors. Although the number of blood granulocytes was higher in LXR-DKO mice in agreement with previous work[16], no major defects in the frequency of BM or peripheral blood monocytes and myeloid progenitors were observed in LXR-DKO mice compared to wild-type controls (Supplementary Fig. 3). Next, we generated hematopoietic chimeras by transplanting bone marrow (BM) from either wild-type or LXR-DKO donors into irradiated wild-type and LXR-DKO recipients. Development of MZ macrophage populations was observed in LXR-DKO mice reconstituted with wild-type BM but not with LXR-DKO BM (Fig. 2c). Moreover, transplantation of LXR-DKO BM into wild-type mice led to an important disruption of the MZ microenvironment (Fig. 2c). These findings strongly suggest that the absence of MZ macrophages in LXR-DKO mice results from an intrinsic hematopoietic defect.

MZ B cells and capture of blood-borne antigens

Previous work suggested that crosstalk between MZ macrophages and a population of non-recirculating MZ B cells was important for the retention and function of both cell types in the spleen[21–23]. MZ B cells are characterized by their localization and $CD1d^{+}$ IgM^{hi} $CD21^{hi}$ $CD23^{lo}$ IgD^{lo} expression pattern[10]. To evaluate the impact of MZ macrophage loss on MZ B cell localization and frequency, wild-type and LXR-DKO spleen sections or cell suspensions were compared by immunofluorescence, immunohistochemistry and flow cytometry analysis. The fraction of $B220^{+}CD21^{hi}CD23^{lo}$ MZ B cells was reduced in LXR-DKO spleen cells compared to wild-type controls (Fig. 3b). Surprisingly, the $B220^{+}CD1d^{+}IgM^{hi}$ B cell population (which normally resides outside the white pulp), was confined to the inner border of the follicles in LXR-DKO spleens (Fig. 3a). Since MZ B cells have been functionally linked to immune responses against thymus-independent (TI) antigens[8, 10], we evaluated the response of wild-type and LXR-DKO mice to trinitrophenyl (TNP)-conjugated Ficoll type-2 TI antigen. IgM titers in response to TNP-Ficoll immunization were significantly reduced in LXR-DKO mice compared to wild-type controls (Fig. 3c). These results indicate that LXR

signaling is important for the retention of MZ B cells within their splenic anatomical compartment and also participates in early IgM responses to TI antigens.

Because a rapid clearance of blood-borne antigens by MZ macrophages is important to prevent dissemination of potentially harmful agents, we investigated the ability of LXR-DKO mice to recognize and clear blood antigens in the absence of MZ macrophages. A panel of intravenously injected bacterial or yeast components, inactivated microorganisms and opsonized particles were efficiently captured by splenic macrophages and generally colocalized with MZ macrophages in wild-type mice. By contrast, circulating antigens aberrantly percolated into the RP of LXR-DKO mice and appeared widely dispersed and associated with F4/80+ macrophages (Fig. 4a, b and Supplementary Fig. 4). These data show that intact LXR signaling is required for the generation of an efficient network of scavenging macrophages in the spleen.

Development of MZ macrophages is dependent on LXRα signaling

To determine if the MZ macrophage defect observed in LXR-DKO mice was dependent on one of the two LXRs, sections from wild-type, *Nr1h3*$^{-/-}$ (LXRα-KO), *Nr1h2*$^{-/-}$ (LXRβ-KO), or LXR-DKO spleens were analyzed by a combination of immunofluorescence and immunohistochemistry approaches. Surprisingly, LXRα-KO mice exhibited a selective ablation of MZ macrophages that was virtually identical to that observed in LXR-DKO mice (Fig. 5a, top). Moreover, immunohistochemistry and immunofluorescence analysis revealed that the establishment of the MZ space between the WP and RP areas was also LXRα-dependent (Fig. 5a, middle and bottom and Supplementary Fig. 5). Consistent with these observations, transplantation of LXRβ-KO BM into LXR-DKO recipients led to a recovery of the MZ space and MZ macrophages, whereas LXRα-KO donor BM could not rescue the MZ microarchitecture (Fig. 5b top, middle). Moreover, transplantation of LXRβ-KO BM (but not with LXRα-KO) into LXR-DKO mice restored the efficient capture of blood-borne antigens and the induction of IgM responses coinciding with the replenishment of MZ macrophages (Supplementary Fig. 6). Interestingly, reconstitution with BM from either LXRα-KO or LXRβ-KO donors reduced neutral lipid accumulation in LXR-DKO spleens, indicating that, while LXRα is uniquely required for the development of MZ macrophages, regulation of cholesterol metabolism in the spleen can be controlled by either LXRα or LXRβ (Fig. 5b bottom).

To confirm the importance of hematopoietic LXRα signaling in the generation of MZ macrophages, we used Cre-lox technology to create a conditional knockout mouse line with selective ablation of LXRα in hematopoietic cells (Supplementary Fig. 7). Mice homozygous for the *Nr1h3* floxed allele (*Nr1h3*$^{fl/fl}$) were crossed with transgenic mice expressing Cre Recombinase under the control of *Vav1* promoter (Vav-Cre)[24]. LXRα deletion efficiency in *Nr1h3*$^{fl/fl}$/Vav-Cre^{+} (hematopoietic LXRα knockout, Hem-LXRα KO) was greater than 95% at the mRNA level in BM and spleen (Supplementary Fig. 7b). Expression of the LXRα-specific target *Cd5l*[25] was used as an additional control of LXRα activity. Immunoblot analysis using an LXRα specific antibody[26] (Supplementary Fig. 8) confirmed a high degree of LXRα deletion in macrophages and in the spleen (but only minimally affected in the liver) of Hem-LXRα KO mice (Fig. 6a top and Supplementary

Fig. 7b). Development of F4/80+ RP macrophages was unaffected in Hem-LXRα KO mice, but there was a complete loss of MZ macrophages (Fig. 6a, bottom).

To gain insight into the cellular mechanisms controlled by LXRα signaling that lead to the development of MZ macrophages, we overexpressed LXRα in hematopoietic stem cells (HSCs) using a myeloid specific lentiviral system[27,28]. First, we examined the expression of the green fluorescent protein (GFP) in blood monocytes obtained from mice transplanted with HSC-enriched BM cells that were previously transduced with the myeloid specific lentivirus. Eight to twelve weeks after transplant, around 40% of monocytes were GFP+ (Fig. 6b top and data not shown). Next, we used lentivirus expressing GFP (Lenti-GFP) or LXRα (Lenti- LXRα) to transduce HSC-enriched BM cells obtained from LXRα-KO donor mice and performed reconstitution studies in a cohort of LXRα-KO recipient mice. Analysis of spleen sections revealed a partial recovery of CD169, MARCO and Tim-4 expressing cells in the MZ compartment in mice transplanted with Lenti-LXRα transduced cells (Fig. 6b). These results indicate that LXRα expression in hematopoietic cells is important for the generation of MZ macrophages.

Wild-type monocytes replenish MZ macrophages in LXRα-KO mice

Although it is generally assumed that BM-derived monocytes give rise to macrophages *in vivo*[4], a direct link between emigrated monocytes and the differentiation of splenic MZ macrophages under steady-state conditions has not yet been established[5]. We evaluated whether the frequency of the classical $CD115^{+}Ly6C^{hi}$ and the nonclassical $CD115^{+}Ly6C^{lo}$ monocyte subsets might be altered in LXRα-KO mice. Flow cytometry analysis demonstrated that $CD115^{+}Ly6C^{hi}$ and $CD115^{+}Ly6C^{lo}$ populations were present at similar frequencies in BM and blood of wild-type and LXRα-KO mice (Fig. 7a). Surprisingly, an increase in splenic monocytes was observed in LXRα-KO mice, an effect that was restricted to the nonclassical $CD115^{+}Ly6C^{lo}$ subset (Fig. 7a). Thus, the absence of MZ macrophages in these mice cannot be accounted by the absence of monocytic precursors.

Next, we tested the potential of mature monocytes to drive the generation of MZ macrophages under steady-state conditions. We first analyzed the ability of i.v.-transferred (DsRed+ or GFP+) BM or splenic monocytes to arrive at representative target tissues of recipient mice. Although each monocyte presented a preferential tropism for their source tissue, both BM and spleen donor monocytes were able to home to the spleen of recipient mice at comparable rates (data not shown). Purified wild-type BM or spleen monocytes ($CD115^{+}CD11b^{+}$ donor cells) were then evaluated for their potential as MZ macrophage precursors in adoptive transfer experiments in nonirradiated LXRα-KO recipient mice. Notably, twelve weeks after transfer, both spleen or BM monocytes from wild-type donors partially reconstituted $CD169^{+}$ and $MARCO^{+}$ cells in the MZ space of LXR-KO mice (Fig. 7b). Additional transfer experiments demonstrated that monocyte-dependent replenishment of MZ macrophages in LXR-DKO mice leads to a partial recovery of the MZ B-cell compartment (data not shown). Together, these data suggest that monocytes coming from the circulation can generate MZ macrophages that are functionally competent.

Because $Ly6C^{hi}$ and $Ly6C^{lo}$ monocytes have been proposed to play distinct roles in inflammation[6], we used our LXRα-KO model to investigate whether these monocyte

subsets exhibited differential capacity to generate MZ macrophages. BM $CD115^{+}CX3CR1^{lo}$ and $CD115^{+}CX3CR1^{hi}$ monocytes (corresponding to $Ly6C^{hi}$ and $Ly6C^{lo}$ subsets, respectively) promoted the development of MZ macrophages with similar efficacy (Supplementary Fig. 9a). Furthermore, purified $Ly6C^{hi}$ and $Ly6C^{lo}$ spleen monocytes showed equivalent mRNA expression of LXRα, LXRβ and ABCA1 (but not CCR2 which was used as a control to distinguish $Ly6C^{hi}$ and $Ly6C^{lo}$ monocytes; Supplementary Fig. 9b). These results suggest that classical and nonclassical monocytes may play redundant roles in the differentiation of certain macrophage subsets under steady-state conditions. However, since $Ly6C^{hi}$ have been shown to generate $Ly6C^{lo}$ monocytes[29, 30], we cannot exclude that $Ly6C^{lo}$ monocytes are the immediate precursors of MZ macrophages in LXRα-KO mice in our experimental model.

Activation of LXRα accelerates MZ macrophage development

Scattered macrophages can be detected during the late phases of embryonic development of the murine spleen, but the organization and specialization of separate splenic macrophage compartments occurs during the first weeks after birth[7, 8]. We studied the expression of macrophage markers in wild-type and LXR-deficient mice during the postnatal transition of the spleen until completion of its full mature appearance. Examination of spleen sections obtained from mice of 1–4 weeks of age revealed that, despite equivalent frequency of F4/80 and CD68 expressing cells, MZ macrophages did not appear during spleen development in LXR-DKO mice (Fig. 8a and data not shown). Thus, LXR signaling is selectively required for the differentiation of MZ macrophages during the maturation of the spleen. Interestingly, postnatal development of MZ macrophage subpopulations correlated with a 10–12 fold increase in LXRα mRNA expression and no changes in LXRβ expression (Fig. 8b).

Finally, we tested the effect of genetic or pharmacological activation of LXRα on the development and function of MZ macrophages. Analysis of three-week old spleen samples from transgenic mice expressing constitutively active VP16-LXRα in macrophages and adipocytes (aP2-VP16LXRα[31]) revealed an accelerated formation of the MZ microenvironment with increased numbers of MZ macrophages found in their mature position compared to wild-type controls (Fig. 9a). Consistent with these histological changes, more SIGN-R1 and CD169 as well as the established LXR target ABCA1, was expressed in the spleens aP2-VP16LXRα mice (Fig. 9a). Since aP2 expression in monocytes is restricted to $Ly6C^{lo}$ monocytes[32], it is possible that VP16-LXRα activity in the $Ly6C^{lo}$ subset contributes to accelerated MZ macrophage formation in this model. We also evaluated whether LXR activity is important for the functions of the MZ compartment by using the synthetic LXR agonist GW3965 *in vivo* in three different assays: Dextran-FITC phagocytosis, IgM response to TNP-Ficoll, and generation of MZ-B cells. Analysis of these activities in wild-type mice did not show differences between the agonist-treated mice and the control group (data not shown), indicating that supraphysiological activation of LXR does not alter MZ macrophage functions in adult mice. We also investigated whether pharmacological activation of LXRα altered the replenishment of splenic macrophages after experimental depletion of tissue macrophages with clodronate-containing liposomes (Clo-lip). This acute depletion of phagocytes provides a model to analyze the progressive renewal of splenic macrophages in adult mice[33], a process that requires 6–8 weeks for full

restoration of all subtypes (data not shown). We then used this Clo-lip model combined with administration of the dual LXR agonist GW3965 in LXRα-KO or LXRβ-KO mice in order to activate exclusively LXRβ or LXRα, respectively. Mice treated i.v. with Clo-lip exhibited a general depletion of splenic macrophages 48h post-treatment as expected[33]. Separate cohorts of LXRα-KO or LXRβ-KO mice were allowed to recover for 2 weeks after Clo-lip injection and then treated for one additional week with the synthetic LXR ligand GW3965 or vehicle control. Activation of LXRβ was unable to promote the development of MZ macrophages in the absence of LXRα. In contrast, activation of LXRα increased the frequency of CD169+ and MARCO+ MZ macrophages compared to control-treated animals. Replenishment of F4/80+ macrophages was not altered by LXRα or LXRβ activation under these conditions (Fig. 9b). Interestingly, because activation of LXRα did not promote the expression of MZ markers in other splenic subsets (Fig. 9b), our results suggest that specific signals at the interface of the WP and RP are also required for the generation of MZ macrophages. Collectively, our results establish that LXRα is crucial for the generation of a specific subset of splenic phagocytes under developmental or homeostatic conditions.

Discussion

Tissue macrophages are a heterogeneous group of cell subsets found in all organs that exhibit distinct surface markers and specialized functions depending on the local microenvironment[1, 4, 5]. Several transcription factors, including PU.1, C/EBPα and Klf4 play important roles in the differentiation of the monocyte/macrophage lineage *in vitro* and *in vivo*[6]. However, genetic models lacking these factors often exhibit profound effects on multiple cell types. Thus, the transcriptional programs that control the generation of particular resident macrophage subsets are largely unexplored. We have shown here that myeloid LXRα signaling is directly involved in the development of specific macrophage subsets important for the efficient capture of circulating antigens. To our knowledge, LXRα is the first gene shown to be selectively required for the development of all MZ macrophages in the steady-state. Our data illustrates a new physiological role for LXRα in myeloid cells driving the differentiation of splenic MZ macrophages. LXRα signaling in monocytes or myeloid progenitors is required for the production of MZ macrophages not only during the neonatal development of the spleen but also throughout the continuous renewal of these cell subsets in adult life.

Loss of MZ macrophages in LXR-deficient mice leads to a number of consequences for spleen architecture and physiology. First, a profound reduction of the MZ space between the RP and the WP affects the retention of MZ B-cells that unexpectedly relocalize to the inner part of the follicle in LXR-deficient mice. Although reciprocal crosstalk between myeloid and B-cells was previously reported to maintain MZ integrity[21–23], our data suggest that the LXRα-dependent development of MZ macrophages provides lodging signals for the entire MZ niche. Second, we showed that efficient clearance of circulating particles and pathogens requires LXR signaling, further emphasizing the importance of MZ macrophages in the recognition and uptake of blood-borne antigens. Our data strongly suggest that loss of MZ macrophages and misplaced MZ B-cells in LXR-deficient mice constitute a permissive environment for many circulating pathogens.

Consistent with an inadequate recognition of circulating antigens, the early IgM antibody response to TNP-Ficoll was impaired in LXR-deficient mice. Because the expression of marginal sinus endotelial markers is normal in LXR deficient mice, we conclude that the vascular network develops properly in these animals. As a consequence, blood arriving from the central arterioles is directly drained into the RP and possibly reaches other tissues with uninspected material. It is likely that the MZ macrophage deficiency described here contributes to the susceptibility to *Listeria monocytogenes* (LM) or *Mycobacterium tuberculosis* infection models observed in LXRα-KO mice[25, 34]. Together with previous studies, we propose that LXRα signaling represents an integral component of the systemic antimicrobial immunity, at least in part, through the regulation of splenic MZ macrophage development.

Although the relevance of tissue macrophage diversity has been recognized for decades[4, 35], the origin of mononuclear phagocyte cells has recently received considerable attention[5, 6]. Whether tissue resident macrophages derive from common hematopoietic precursors or from yolk sac-derived precursors is a matter of intense research[29, 30, 36–39]. There is also evidence that demonstrates that macrophages can self-renew locally independently of their bloodstream precursors[5, 40]. Although similar questions relate to the origin and renewal of splenic murine macrophages[33, 41], further complexity applies due to the number of different resident subsets in this tissue and the fact that the spleen continues to function as a hematopoietic organ in adult rodents. Our results provide the first demonstration that a single nuclear receptor controls the differentiation of the splenic MZ macrophage population through a myeloid-restricted signaling.

Several lines of evidence suggest that absence of MZ macrophages in LXR−/− mice results from a defective sub-lineage developmental step. Bone marrow transplant or hematopoietic LXRα conditional-knockout experiments indicate that LXRα-expressing myeloid cells give rise to MZ macrophages. A complementary gain of function approach with a macrophage-specific lentivirus confirmed that LXRα expression in myeloid cells is necessary to reprogram target cells with the appropriate MZ differentiating potential *in vivo*. These data also imply that the development and organization of RP and WP macrophages in the spleen take place independently of the formation of the MZ and of LXRα signaling. Interestingly, recent studies demonstrated that differentiation of F4/80+ macrophages is impaired in *Spic* −/− mice while MZ macrophages in these mice develop normally[42]. We interpret the correlation between LXRα expression and splenic macrophage compartmentalization as a strong evidence that supports the existence of a separate pathway controlling the generation of MZ macrophages.

Although monocytes contribute to increased tissue macrophage levels in several pathological settings[43], the monocytic origin of resident macrophages in the steady-state has not been clearly established. We have shown that adoptively transferred wild-type monocytes partially reconstituted the MZ microenvironment in LXRα-KO mice. Whereas classical and nonclassical monocytes play distinct roles in inflammation[6, 44], the ability of monocytes to replenish a vacant MZ microenvironment in LXRα-KO mice under homeostatic conditions can be accomplished by both $Ly6C^{hi}$ and $Ly6C^{lo}$ monocytes. Our data indicate that either circulating monocytes or local splenic monocytes can function as

MZ macrophage precursors under conditons of LXRα deficiency. Our findings do not exclude the possibility that MZ macrophages in wild-type mice may derive from embryonic precursors under homeostasis without contributions from circulating monocytes, as demonstrated for other tissue-resident populations[30, 36, 39].

Finally, we found that enhancement of LXRα activity during macrophage renewal in mature mice led to an accelerated MZ macrophage differentiation program. Thus, intrasplenic induction and activation of LXRα in myeloid cells is crucial for the generation and maintenance of MZ macrophages both during development and in adult life. We hypothesize that the instructive signals that drive full maturation of monocytes into MZ macrophages and upregulate LXRα expression in the spleen should be released at the neonatal stage and remain present throughout adult life. Since oxysterols have recently been shown to influence various immune cell functions *in vivo*, including proliferation and migration[45–47], it is tempting to speculate that spleen-specific sterol derivatives play a role in activating LXRα during the development of MZ macrophages. Further studies will be required to characterize such signals and their downstream effects in LXRα-sufficient or -deficient monocytes during the differentiation to splenic macrophages.

Methods

Animals

Mice were maintained under pathogen-free conditions in a temperature-controlled room and a 12-hour light/dark cycle. Chow and water were available *ad libitum*. LXRα,β- wild-type (*Nr1h3*+/+, *Nr1h2*+/+), LXRα-KO (*Nr1h3*−/−), LXRβ-KO (*Nr1h2*−/−) and LXR-DKO (*Nr1h3*−/−, *Nr1h2*−/−) mice on a mixed Sv129/C57Bl/6 and C57Bl/6 (backcrossed more than ten generations) backgrounds were originally obtained from David Mangelsdorf (UTSW)[48]. Mice bearing a floxed allele of LXRα (*Nr1h3*$^{fl/+}$) on a C57Bl/6 background were obtained from Institut Clinique de la Souris (Illkirch, France); transgenic C57Bl/6 Vav-Cre mice were obtained from D. Kioussis[24] (NIMC, UK) through a collaboration with Susana Gonzalez (CNIC, Spain); transgenic mice expressing constitutively active VP16-LXRα in macrophages and adipocytes (aP2-VP16LXRα) have been described[31]; *Cx3cr1*$^{GFP/+}$ knock-in mice and transgenic mice expressing GFP or DsRed under the control of the β-actin promoter were obtained from the Jackson Laboratory. All animal studies were conducted in accordance with the CSIC and ULPGC Animal Research Committees.

Reagents and antibodies

The LXR (GW3965) and RXR (LG268) synthetic ligands were kindly provided by Jon Collins and Tim WIllson (GlaxoSmithKline SA). The following antibodies and conjugates were used in this study: Anti-MAdCAM-1 clone MECA-367 and anti-SIGN-R1 clone 22D1 were obtained from the ATCC; anti-CD45R B220 clone RA3-6B2, anti-CD62L-FITC, anti-CD11b purified and FITC conjugated Clone M1/70, anti-Ter119-FITC, anti-CD117-FITC, anti-CD1d (clone 1B1), anti-VCAM-1 (clone 429), anti-CD21-PE (clone 7G6), and anti-CD23-FITC (clone B3B4) were from BD Biosciences, anti-Tim-4-PE (clone RMT4-54), anti MHC-II clone I-Ab, anti-IgD-FITC (clone 11-26c) were from from eBioscience; anti-CD68 clone FA-11, anti-MOMA-1-FITC, anti-MARCO clone ED31 were from Serotec;

anti-F4/80 clone Cl:A3-1 and anti CD169 clone 3D6 were kindly provided by S. Gordon and M. Stacey (U. Oxford, UK); anti TremL4 was obtained from R. Steinman lab (Rockefeller NY) through Gwen Randolph (Washington University); anti-FDC-M1 and M2 were kindly provided by M. Kosco-Vilbois (Novimmune SA); anti-IgM-PE and anti-IgM-HRP from Southern Biotech; anti-mouse Laminin from Sigma; anti-Ly6C-PerCP-Cy5.5 clone HK1.4 and anti-CD115-PE clone AFS98 and purified anti-Tim-4 clone RMT4-54 were from Biolegend; a Lineage cell detection cocktail containing biotinylated CD5, CD11b, CD45R, 7/4, Gr-1 and Ter-119 antibodies was obtained from Miltenyi Biotec. Alexa Fluor 488-anti-rat-IgG and IgM, Alexa Fluor 594- anti-rat-IgG and IgM, Alexa Fluor 350-anti rat-IgG (Molecular Probes), and anti-rat biotin antibody (Dako Cytomation).

Flow cytometry and progenitor assays

Bone marrow cells were obtained from femurs and tibiae by flushing with culture media. Blood cells were obtained by collecting EDTA-treated blood samples. Spleen cells were obtained using a GentleMACS dissociator and a mouse spleen dissociation kit according to the manufacturer instructions (Miltenyi Biotec). In all cases single-cell suspensions were obtained and erythrocytes lysed using a hypotonic buffer. Cells were washed and resuspended in PBS with 0.1% BSA and 0.1% sodium azide. Single cell suspensions were stained for 30 minutes at 4°C with the indicated antibodies. Cells were then analyzed on Beckman Coulter Epics XL, BD FACS Canto-II, BD FACS-Vantage or BD FACS-Aria with FlowJo software (Treestar). Monocytes were identified as CD115+CD11b+F4/80^{int} and Ly6C^{hi} or Ly6C^{lo}. Splenic phagocytes were detected by the expression of MHCII, F4/80, CD68 and Tim-4 antigens. MDPs (macrophage DC progenitor) were identified as Lineage^{Neg}CD117^{+}CD115^{+}. Blood counts were obtained using an Abacus automated hematological counter (Diatron, USA). Colony-forming units in culture (CFU-C) assays were determined in blood and BM samples. Briefly, blood and BM were collected and diluted in Lympholyte solution (Cedarlane Labs) and centrifuged to obtain mononuclear cells. Cells were cultured in semisolid media containing 1.25% methylcellulose (Sigma-Aldrich), 30% FBS (StemCell Technologies), 1% BSA, 0.1mM 2-mercaptoethanol, and conditioned medium (12.7% v/v) from the WEHI3 cell line (expressing IL-3), HM-5 cell line (expressing GM-CSF) and BHK/MKL cell line stably transfected to produce KitL. Cultures were plated in duplicates in 35 mm culture dishes and the numbers of CFU-Cs were scored on day 6 or 7 using an inverted microscope.

Histology

Tissues were collected and fixed in 4% buffered formalin, dehydrated in successive alcohol solutions, embedded in paraffin wax, and sectioned for H&E staining. Alternatively, tissues were directly collected from the animal, embedded in OCT compound (Tissue-Tek), and snap-frozen in liquid Nitrogen and Isopentane. 4 μm frozen sections were air-dried, fixed with cold acetone, blocked with 6% BSA and 2% preimmune serum in PBS, and stained with fluorescence-conjugated antibodies diluted in blocking solution; nuclei were stained with DAPI (Vectashield mountain medium fluorescence with DAPI, Vector). Primary purified antibodies were also detected by Alexa-Fluor secondary antibodies (Molecular Probes). For non-fluorophore-conjugated antibodies, biotinylated secondary antibodies were visualized by the streptavidin-biotin-peroxidase method (Vectastain ABC Kit, Vector

Laboratories) and stained with the cromogen 3-30-diaminobenzidine tetrahydrochloride DAB or Alkaline Phosphatase (DAB HRP or Vector Blue Substrate Kits, Vector Laboratories). Nuclei were counterstained with hematoxilin or Methyl green (Sigma). Sections were observed under a Zeiss LSM 5 PASCAL Laser Scaning Microscope (Carl Zeiss, Germany) or Eclipse Nikon 90i (Nikon).

For transmission electron microscopy analysis, LXR wild-type and DKO mice were sacrified and perfused with fixation solution (2% glutaraldheyde). Spleens were fixed with 2% OsO_4, dehydrated and embedded in epoxy resin. Ultra-thin sections were stained with uranyl acetate and lead citrate and observed under elctron microscope at the ULPGC electron microcopy core facilty.

In vivo treatments

For antigen capture of circulating antigens, the following reagents were used: labeled high molecular weight dextran, inactivated *Staphylococcus aureus*, Zymosan were obtained from Life Technologies; GFP labeled *Escherichia coli* had been previously described[15]; platelets were purified by centrifugation of whole blood in Citrate-phosphate-dextrose solution. A platelet-rich plasma was collected and washed with PBS. Platelets were opsonized with 5μg anti-mouse CD41 antibody (clone MWReg30 from BD Biosciences). Antigens were intravenously injected into wild-type and LXR deficient mice for a 30 minute period. Spleens were harvested and tissues were prepared for immunofuorescence analysis as detailed above.

For liposome-mediated depletion of splenic macrophages, mice were injected intravenously with Clodronate (Cl_2MBP; dichloromethylene-biphosphonate)-loaded liposomes or control PBS liposomes (obtained from Encapsula Nanosciences) in 200μl suspension solution. Mice were sacrified at the indicated times and tissues were harvested for histological analysis. For LXR ligand treatment *in vivo* after macrophage depletion with clodronate liposomes, GW3965 stock solution was diluted in PBS and injected 20mg/kg intraperitoneally every 2 days for one week. Mice were sacrified and total RNA was prepared 2h after the last injection of ligand.

Bone marrow transplant and adoptive transfer studies

For bone marrow transplants, recipient wild-type and LXR-DKO mice (6–8 weeks of age) were lethally irradiated with 900 rads and transplanted with 3×10^6 bone marrow cells from 6–8 week-old donors (wild-type, LXRα-KO, LXRβ-KO or LXR-DKO) by retro-orbital injection. Recipient mice were sacrified at 8–12 weeks after transplantation and spleen sections were then analyzed for the presence of macrophages as detailed above.

For adoptive transfer experiments, total monocytes from bone marrow or spleen were sorted on a FACS-Vantage or FACSAria (BD Biosciences) as $CD11b^{hi}$, $CD115^{hi}$ and purity was greater than 90%. Cells were intravenously injected ($2–3\times 10^6$ cells) into non-irradiated LXRα-KO mice. Recipient mice were sacrified at 8–12 weeks post-injection and spleens were processed as described above. For homing experiments, unfractioned splenocytes or bone marrow cells from GFP or Ds-Red transgenic animals were coinjected intravenously

into wild-type recipient mice. Target tissues were processed and the relative homing of GFP and Ds-Red positive monocytes was analyzed 24hr post-injection by Flow Cytometry. In other set of experiments, monocytes were purified from bone marrow or spleen from *Cx3cr1*$^{GFP/+}$ knock-in mice. Classical CD115^{+}CX3CR1^{lo} and nonclassical CD115^{+}CX3CR1^{hi} monocytes were transferred (1–2×10^{6} cells) to LXRα-KO mice. Spleens were isolated and analyzed by immunofluorescence as detailed above.

Lentivirus production and infection of HSC-enriched BM cells

A lentiviral system containing a macrophage-specific synthetic promoter (SP) was previously described in the laboratory of S. Li[27]. Briefly, Lenti-SP-GFP or Lenti-SP-LXRα constructs, were transfected with pMDlg-pRRE, pRSV/Rev and pMD2G in HEK-293 cells with FuGENE-HD (Promega). After 48h, supernatant was collected and viral particles were centrifuged at 86000xg on a SW41Ti swing bucket rotor (Beckman). Pellets were resuspended in StemPro 34 SFM 1%L-Glut+1%Pen+Strep and concentration of lentiviral particles was determined by flow cytometry analysis of transduced RAW264.7 cells with serially diluted lentiviral particles. To prepare cells for lentiviral transduction, total BM cells were enriched for HSCs by using the EasySep Hematopoietic progenitor enrichment kit (StemCell Technologies) or by treating donor mice with 5-Fluorouracil for four days. HSC-enriched cells were resuspended in StemPro-34 media supplemented with 10ng/ml of IL-3, IL-6, IL1α and mSCF for 18 hours. Cells were then infected with Protamine Sulfate-treated Lenti-SP-LXRα or Lenti-SP-GFP viral particles for 24 hours. Eight hours before transplantation, recipient mice were irradiated as described above. Transduced HSC cells were resuspended in PBS and injected intravenously (2 × 10^{6}) into LXRα-KO recipient mice together with a fraction of LXRα-KO total BM cells (5 × 10^{5}). After 8–12 weeks mice were sacrified and blood and spleens were collected and tissues were processed for histology as described above.

Immunization and IgM determination by ELISA

To evaluate the T-independent IgM response, wild-type and LXR-DKO mice were immunized by intrevenous injection of 100ug of TNP-Ficoll (Biosearch Technologies). Serum samples were obtained before injection and on days 4 and 7 after immunization with TNP-Ficoll. 96-well flat-bottom plates (Nunc-immuno plate F96 MAXISORP) were precoated with poly-L-lysine (Sigma) for 1 hr at 37°C in a humidified chamber and were incubated 18hr at 4°C with a solution containing TNP-BSA as capture antigen (25ug/ml). After blocking the nonspecific sites with PBS containing 2% FBS and 1% BSA for 1 hr at 37C, serial dilutions of serum samples were added for 2 hr at 20–25°C. Wells were then washed with PBS plus 0.05% Tween-20, and incubated with horseradish peroxidase-conjugated goat anti-mouse IgM (diluted 1:500, Southern Biotechnology). Wells were developed with TMB substrate solution (3,3′,5,5′-tetramethylbenzidine). After incubation of 5 min at 20–25°C, reaction was stopped with 50 μl of 3M H2SO4 solution and the optical density was measured at 450 nm in ELISA plate reader (Bio-Rad).

DNA, RNA, and Protein Analysis

Total RNA was harvested with TRIzol reagent (Invitrogen). RNA was reverse-transcribed using iScript reverse-transcription kit (Bio-Rad). Real-time quantitative PCR (SYBRgreen) assays were performed with an Applied Biosystems 7900 sequencer detector as described previously[15]. Expression was normalized to 36B4 expression. Primer sequences are included in the supplemental material (Supplementary Table 1). Genomic DNA for genotyping was obtained from mouse tails with a PureGene mouse tail kit from Qiagen. Primers and PCR specifications for *Nr1h3* floxed or iVav-Cre alleles were obtained from Institut Clinique de la Souris and S. Gonzalez (CNIC) respectively (Supplementary Table 1). For immunoblot analysis, peritoneal macrophages and RAW264.7 or HeLa cells stably overexpressing LXRα were cultured as described previously[15]. Whole cell lysates were obtained with RIPA buffer, boiled and separated on a SDS-PAGE gel. Proteins were transferred onto polyvinylidene difluoride membrane (Amersham), blocked in TBS with 0.1% Tween20 and 5% milk, and incubated with the indicated antibodies. Anti-LXRα monoclonal antibody (clone PPZ0412, AbCAM) and anti-ABCA1 polyclonal antibody (NB400-105 Novus Biologicals) were used at 1:1000 and 1:3000 dilutions respectively. Blots were washed in TBS-T and visualized with ECL-Plus (Amersham Biosciences) and Bio-Rad Chemi-Doc imaging system.

Statistical Analysis

Data were expressed as mean ± SEM. Statistical analysis was performed with Student's t test for two samples. For multiple comparisons, data were evaluated by one-way analysis of variance (ANOVA). Values of $p < 0.05$ were considered to be significant.

Supplementary Material

Refer to Web version on PubMed Central for supplementary material.

Acknowledgments

We thank D. Mangelsdorf (University of Texas Southwestern) for the LXR null mice, the Institut Clinique de la Souris for LXRα floxed mice and D. Kioussis (MRC, UK) and S. Gonzalez (CNIC, Spain) for iVav-Cre mice; we also thank S. Gordon (University of Oxford), N. Ruddle (Yale University), G. Randolph (Whashington University in St. Louis), C. Glass and N. Spann (University of California San Diego), A. Chawla (University of California San Francisco), G. Lemke (Salk Institute), D. Hume (The Roslin Institute), L. Hedrick (LIAI San Diego), A. Lazarus (Keenan Research Centre, Toronto), M. Kosco-Vilbois (NovImmune SA, Geneva), J. Collins (GlaxoSmithKline SA North Carolina) and L. Bosca for reagents; Servicio Microscopia Electronica ULPGC for electron microscopy studies. P.T. is an Investigator of the Howard Hughes Medical Institute. This work was supported by the following grants: NIH HL-066088 and HL-030568 to P.T.; Ramon y Cajal fellowship (RYC-2007-00697), SAF2009-11037 and FP7-People IRG246655 to A.H.; Spanish Ministry of I+D 2008-00057, MINECO SAF2011-29244, Comunidad de Madrid I+D Grant S2010/BMD-2350 to A.C. JVdR is supported by a fellowship from Universidad Las Palmas de Gran Canaria. MC-A and IHH are supported by FPI fellowships from the Spanish MINECO.

References

1. Taylor PR, et al. Macrophage receptors and immune recognition. Annu Rev Immunol. 2005; 23:901–944. [PubMed: 15771589]
2. Medzhitov R. Origin and physiological roles of inflammation. Nature. 2008; 454:428–435. [PubMed: 18650913]

3. Elliott MR, Ravichandran KS. Clearance of apoptotic cells: implications in health and disease. J Cell Biol. 2010; 189:1059–1070. [PubMed: 20584912]
4. Gordon S, Taylor PR. Monocyte and macrophage heterogeneity. Nat Rev Immunol. 2005; 5:953–964. [PubMed: 16322748]
5. Hashimoto D, Miller J, Merad M. Dendritic cell and macrophage heterogeneity in vivo. Immunity. 2011; 35:323–335. [PubMed: 21943488]
6. Geissmann F, et al. Development of monocytes, macrophages, and dendritic cells. Science. 2010; 327:656–661. [PubMed: 20133564]
7. Mebius RE, Kraal G. Structure and function of the spleen. Nat Rev Immunol. 2005; 5:606–616. [PubMed: 16056254]
8. Kraal G, Mebius R. New insights into the cell biology of the marginal zone of the spleen. Int Rev Cytol. 2006; 250:175–215. [PubMed: 16861066]
9. den Haan JM, Kraal G. Innate immune functions of macrophage subpopulations in the spleen. J Innate Immun. 2012; 4:437–445. [PubMed: 22327291]
10. Martin F, Kearney JF. Marginal-zone B cells. Nat Rev Immunol. 2002; 2:323–335. [PubMed: 12033738]
11. Repa JJ, Mangelsdorf DJ. The role of orphan nuclear receptors in the regulation of cholesterol homeostasis. Annu Rev Cell Dev Biol. 2000; 16:459–481. [PubMed: 11031244]
12. A-Gonzalez N, Castrillo A. Liver X receptors as regulators of macrophage inflammatory and metabolic pathways. Biochim Biophys Acta. 2011; 1812:982–994. [PubMed: 21193033]
13. Glass CK, Saijo K. Nuclear receptor transrepression pathways that regulate inflammation in macrophages and T cells. Nat Rev Immunol. 2010; 10:365–376. [PubMed: 20414208]
14. Joseph SB, Castrillo A, Laffitte BA, Mangelsdorf DJ, Tontonoz P. Reciprocal regulation of inflammation and lipid metabolism by liver X receptors. Nat Med. 2003; 9:213–219. [PubMed: 12524534]
15. A-Gonzalez N, et al. Apoptotic cells promote their own clearance and immune tolerance through activation of the nuclear receptor LXR. Immunity. 2009; 31:245–258. [PubMed: 19646905]
16. Hong C, et al. Coordinate regulation of neutrophil homeostasis by liver X receptors in mice. J Clin Invest. 2012; 122:337–347. [PubMed: 22156197]
17. Calkin AC, Tontonoz P. Transcriptional integration of metabolism by the nuclear sterol-activated receptors LXR and FXR. Nat Rev Mol Cell Biol. 2012; 13:213–224. [PubMed: 22414897]
18. Streeter PR, Berg EL, Rouse BT, Bargatze RF, Butcher EC. A tissue-specific endothelial cell molecule involved in lymphocyte homing. Nature. 1988; 331:41–46. [PubMed: 3340147]
19. Garin A, et al. Toll-like receptor 4 signaling by follicular dendritic cells is pivotal for germinal center onset and affinity maturation. Immunity. 2010; 33:84–95. [PubMed: 20643339]
20. Hemmi H, et al. A new triggering receptor expressed on myeloid cells (Trem) family member, Trem-like 4, binds to dead cells and is a DNAX activation protein 12-linked marker for subsets of mouse macrophages and dendritic cells. J Immunol. 2009; 182:1278–1286. [PubMed: 19155473]
21. Nolte MA, et al. B cells are crucial for both development and maintenance of the splenic marginal zone. J Immunol. 2004; 172:3620–3627. [PubMed: 15004164]
22. Karlsson MC, et al. Macrophages control the retention and trafficking of B lymphocytes in the splenic marginal zone. J Exp Med. 2003; 198:333–340. [PubMed: 12874264]
23. Lu TT, Cyster JG. Integrin-mediated long-term B cell retention in the splenic marginal zone. Science. 2002; 297:409–412. [PubMed: 12130787]
24. de Boer J, et al. Transgenic mice with hematopoietic and lymphoid specific expression of Cre. Eur J Immunol. 2003; 33:314–325. [PubMed: 12548562]
25. Joseph SB, et al. LXR-dependent gene expression is important for macrophage survival and the innate immune response. Cell. 2004; 119:299–309. [PubMed: 15479645]
26. Watanabe Y, et al. Expression of the LXRalpha protein in human atherosclerotic lesions. Arterioscler Thromb Vasc Biol. 2005; 25:622–627. [PubMed: 15625283]
27. He W, et al. Development of a synthetic promoter for macrophage gene therapy. Hum Gene Ther. 2006; 17:949–959. [PubMed: 16972763]

28. Li G, et al. Macrophage LXRalpha gene therapy ameliorates atherosclerosis as well as hypertriglyceridemia in LDLR(−/−) mice. Gene Ther. 2011; 18:835–841. [PubMed: 21390069]
29. Varol C, et al. Monocytes give rise to mucosal, but not splenic, conventional dendritic cells. J Exp Med. 2007; 204:171–180. [PubMed: 17190836]
30. Yona S, et al. Fate Mapping Reveals Origins and Dynamics of Monocytes and Tissue Macrophages under Homeostasis. Immunity. 2013; 38:79–91. [PubMed: 23273845]
31. Hong C, et al. Constitutive activation of LXR in macrophages regulates metabolic and inflammatory gene expression: identification of ARL7 as a direct target. J Lipid Res. 2010; 52:531–539. [PubMed: 21187453]
32. Ingersoll MA, et al. Comparison of gene expression profiles between human and mouse monocyte subsets. Blood. 2010; 115:e10–19. [PubMed: 19965649]
33. van Rooijen N, Kors N, Kraal G. Macrophage subset repopulation in the spleen: differential kinetics after liposome-mediated elimination. J Leukoc Biol. 1989; 45:97–104. [PubMed: 2521666]
34. Korf H, et al. Liver X receptors contribute to the protective immune response against Mycobacterium tuberculosis in mice. J Clin Invest. 2009; 119:1626–1637. [PubMed: 19436111]
35. van Furth R, Cohn ZA. The origin and kinetics of mononuclear phagocytes. J Exp Med. 1968; 128:415–435. [PubMed: 5666958]
36. Ginhoux F, et al. Fate mapping analysis reveals that adult microglia derive from primitive macrophages. Science. 2010; 330:841–845. [PubMed: 20966214]
37. Fogg DK, et al. A clonogenic bone marrow progenitor specific for macrophages and dendritic cells. Science. 2006; 311:83–87. [PubMed: 16322423]
38. Hoeffel G, et al. Adult Langerhans cells derive predominantly from embryonic fetal liver monocytes with a minor contribution of yolk sac-derived macrophages. J Exp Med. 2012; 209:1167–1181. [PubMed: 22565823]
39. Schulz C, et al. A lineage of myeloid cells independent of Myb and hematopoietic stem cells. Science. 2012; 336:86–90. [PubMed: 22442384]
40. Jenkins SJ, et al. Local macrophage proliferation, rather than recruitment from the blood, is a signature of TH2 inflammation. Science. 2011; 332:1284–1288. [PubMed: 21566158]
41. van Furth R, Diesselhoff-den Dulk MM. Dual origin of mouse spleen macrophages. J Exp Med. 1984; 160:1273–1283. [PubMed: 6491600]
42. Kohyama M, et al. Role for Spi-C in the development of red pulp macrophages and splenic iron homeostasis. Nature. 2009; 457:318–321. [PubMed: 19037245]
43. Swirski FK. The spatial and developmental relationships in the macrophage family. Arterioscler Thromb Vasc Biol. 2011; 31:1517–1522. [PubMed: 21677294]
44. Swirski FK, et al. Identification of splenic reservoir monocytes and their deployment to inflammatory sites. Science. 2009; 325:612–616. [PubMed: 19644120]
45. Hannedouche S, et al. Oxysterols direct immune cell migration via EBI2. Nature. 2011; 475:524–527. [PubMed: 21796212]
46. Bensinger SJ, et al. LXR signaling couples sterol metabolism to proliferation in the acquired immune response. Cell. 2008; 134:97–111. [PubMed: 18614014]
47. Villablanca EJ, et al. Tumor-mediated liver X receptor-alpha activation inhibits CC chemokine receptor-7 expression on dendritic cells and dampens antitumor responses. Nat Med. 2009; 16:98–105. [PubMed: 20037595]
48. Peet DJ, et al. Cholesterol and bile acid metabolism are impaired in mice lacking the nuclear oxysterol receptor LXR alpha. Cell. 1998; 93:693–704. [PubMed: 9630215]

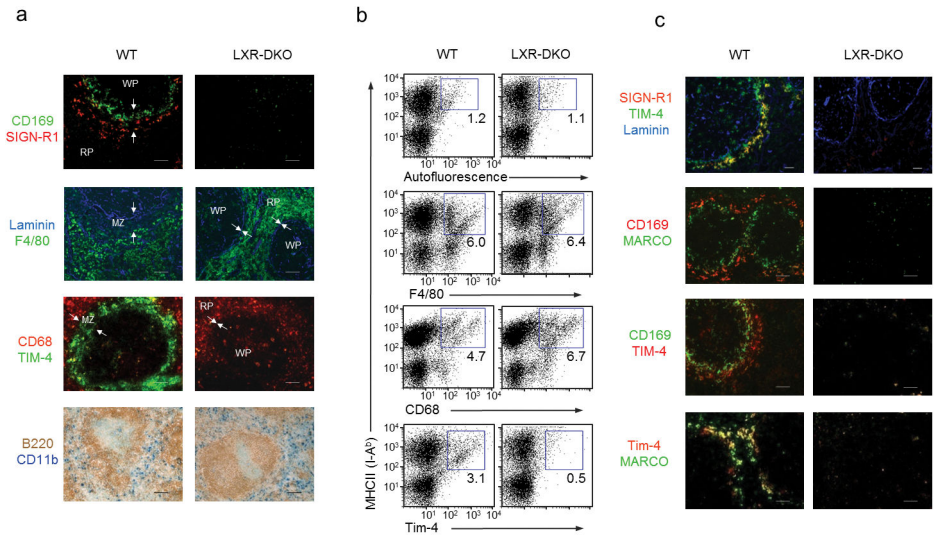

Figure 1. Defective MZ macrophage differentiation in LXR-DKO mice

(a) Top, splenic sections from wild-type (WT) and LXR-DKO mice were stained with specific antibodies that detect CD169+ macrophages (green) and SIGN-R1+ macrophages (red). Below, consecutive sections show RP macrophages (F4/80, green) and stromal endothelial cells (laminin, blue): $CD68^+$ macrophages (red) and $TIM\text{-}4^+$ cells in the MZ (green). Bottom, immunohistochemical analysis of RP $CD11b^+$ cells (blue) and B cells (B220, brown). Arrows indicate the RP and WP borders. Scale bars represent 50 μm. **(b)** Flow cytometry analysis of F4/80, CD68, Tim-4 and MHCII expression in splenic cell suspensions from WT and LXR-DKO mice. Representative plots are shown from three independent experiments with n = 4–5 mice per genotype. Numbers within plots indicate percent of gated cell population **(c)** Immunofluorescence analysis of spleen sections from WT and LXR-DKO mice showing combinations of double or triple stainings with antibodies that recognize MZ macrophages (SIGN-R1, MARCO and Tim-4), marginal metallophillic macrophages (CD169) or endothelial cells (Laminin). Scale bars represent 50 μm. Representative images obtained from five independent experiments with n= 3–5 mice per genotype (**a, c**).

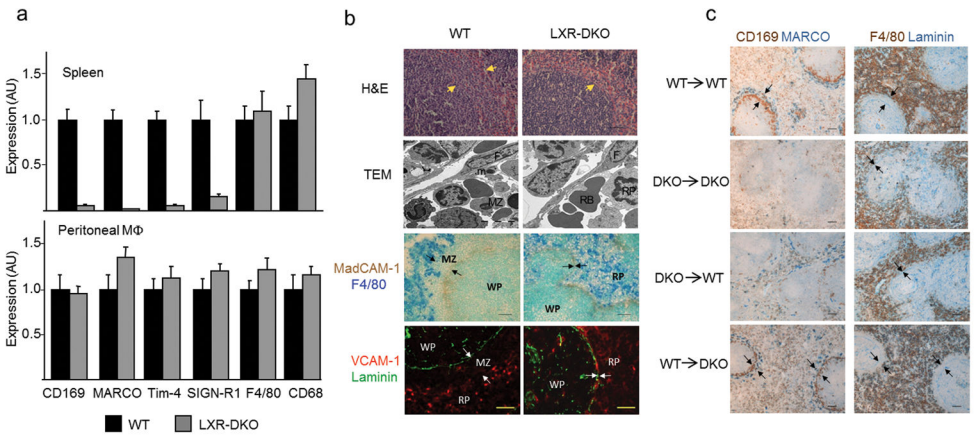

Fig. 2. Generation of MZ macrophages require LXR function in hematopoietic progenitors

(a) Relative mRNA abundance of SIGN-R1, MARCO, Tim-4, F4/80 and CD68 in WT and LXR-DKO spleens (top) and peritoneal macrophages (bottom). Data are normalized to ribosomal protein *Rplp0* (also called 36B4) mRNA expression. Bars indicate mean +/− SEM (n=3 mice). Data are representative of two independent experiments. **(b)** Hematoxilin and eosin staining (top), transmission electron microscopy images (second row); abbreviations: MZ: MZ macrophage; m: marginal metallophilic macrophage; F: follicular reticular cell; RB: red blood cell. RP: RP macrophage. Third row shows immunohistochemical localization of RP F4/80^{+} macrophages relative to MadCAM-1 marginal sinus cells; (bottom row) VCAM-1^{+} cells in the RP relative to laminin^{+} endothelial cells; scale bar represents 30 αm. Arrows indicate RP and WP borders. Representative images obtained from three independent experiments with n = 2–3 mice per group. **(c)** Immunohistochemical localization of RP and MZ compartments in WT and LXR-DKO mice after reciprocal bone marrow transplants. Scale bar represents 50 αm. Arrows indicate the RP and WP borders. Marginal metallophilic macrophages (CD169, brown) and MZ macrophages (MARCO, blue), or RP macrophages (F4/80, brown) and endothelial cells (Laminin, blue) were stained in consecutive spleen sections obtained from mice 12 weeks after BM transplantation (representative images obtained from two independent experiments with n = 5–6 mice per group).

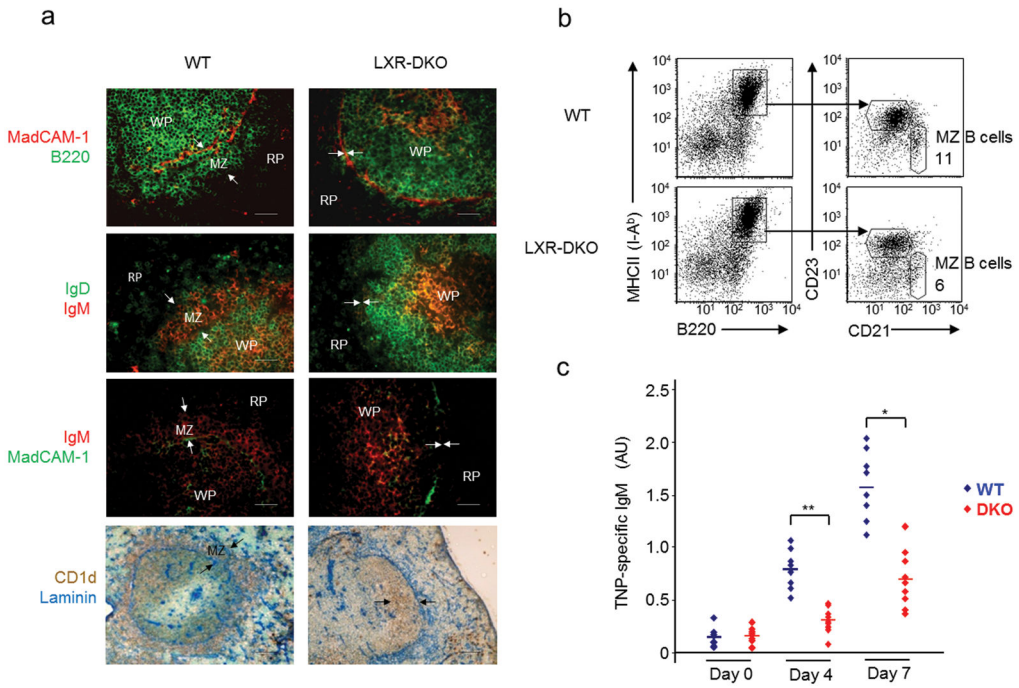

Fig. 3. Analysis of MZ B cell distribution and function

(a) Immunofluorescence and immunohistochemical analysis of spleen sections from WT and LXR-DKO mice stained with antibodies that detect MZ B cells. Top, MZ $B220^{+}$ B cells identified outside the follicles, which are delimitated by MadCAM-1^{+} cells in WT mice and absent in LXR-DKO mice; second row $IgM^{hi}IgD^{lo}$ MZ B cells; third row IgM^{hi} MZ B cells outside MadCAM-1+ sinus lining cells; and bottom CD1d Laminin double immunohistochemical analysis. Arrows indicate the RP and WP borders. Scale bars represent 50 μm. Representative images from n=10 mice per genotype are shown **(b)** Flow cytometry of splenocytes from WT and LXR-DKO mice stained with CD23 and CD21 antibodies and analyzed in gated $B220^{+}$ cells. MZ B cells were quantifed as $CD21^{hi}CD23^{lo}$; representative analysis obtained from three independent experiments of n = 3–5 mice is presented. **(c)** Mice were immunized i.v. with TNP-ficoll and serum samples were obtained before immunization and 4 and 7 days after immunization. TNP-specific IgM titers were measured by ELISA. Representative results obtained from two independent experiments with n = 6–10 mice per group are shown. Each (◆) symbol represents individual WT (blue, n = 8) or LXR-DKO (red, n = 9) mice; $*P < 0.01$ and $**P < 0.001$.

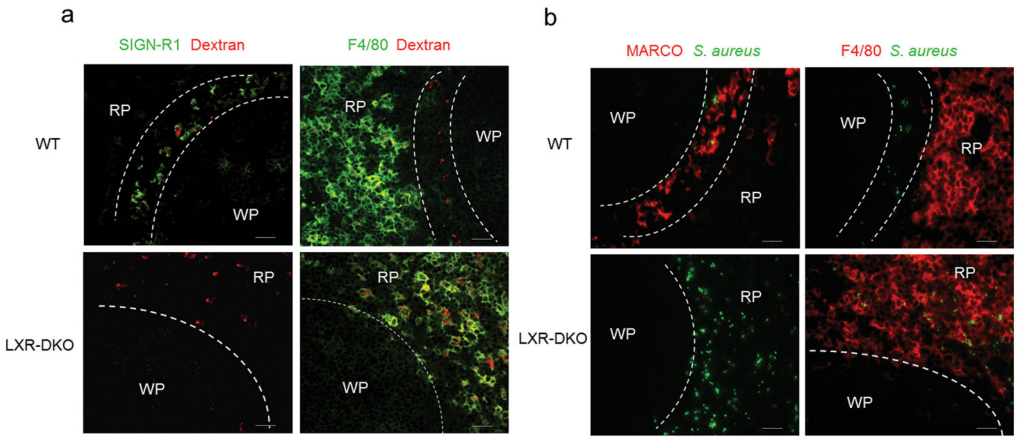

Fig. 4. Abnormal capture of blood-borne antigens by LXR-DKO splenic macrophages

Immunofluorescence microscopy of spleen sections obtained from WT and LXR-DKO mice after 30 min post i.v. injection with dextran-Alexa Fluor 594 **(a)** and Alexa Fluor 488-*Staphyloccocus aureus* particles **(b).** MZ macrophages were detected with SIGN-R1 (green) and MARCO (red) abs in (**a**) and (**b**) respectively. RP macrophages were detected with F4/80 antibody (green in **a**; red in **b**). Dashed lines delimitate the border of the WP and the RP. Scale bar represents 50 μm. Representative pictures from four independent experiments with n = 3–5 mice per group are presented.

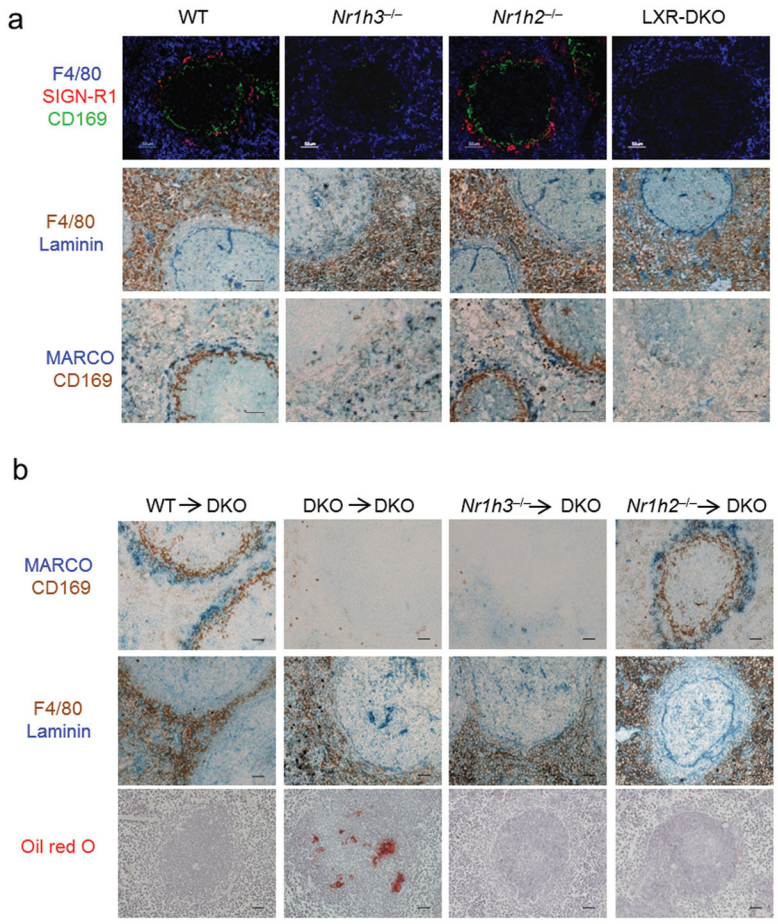

Fig. 5. MZ macrophage differentiation is specifically controlled by LXRα

(a) Top, immunofluorescence analysis of spleen sections from WT, LXRα-KO, LXRβ-KO, and LXR-DKO mice stained with CD169, SIGN-R1 and F4/80 antibodies. Middle, Immunohistochemical analysis of F4/80$^+$ RP macrophages (brown) relative to Laminin$^+$ endothelial cells (blue); bottom, consecutive sections stained for MARCO$^+$ (blue) and CD169$^+$ cells (brown). **(b)** Consecutive spleen sections (top, middle) show immunohistochemical localization of MZ macrophages (MARCO, blue and CD169, brown), and F4/80$^+$ (brown) and Laminin$^+$ endothelial cells (blue) obtained from LXR-DKO mice after transplant experiments with bone marrow from the indicated donor mice. Bottom, Oil-Red O staining in spleen sections from the indicated mice after bone marrow transplantation. Scale bar represents 50 μm. Representative pictures from four independent experiments with *n* = 3–5 mice (panel a) and two independent experiments with n= 6 mice per group (panel b) are presented.

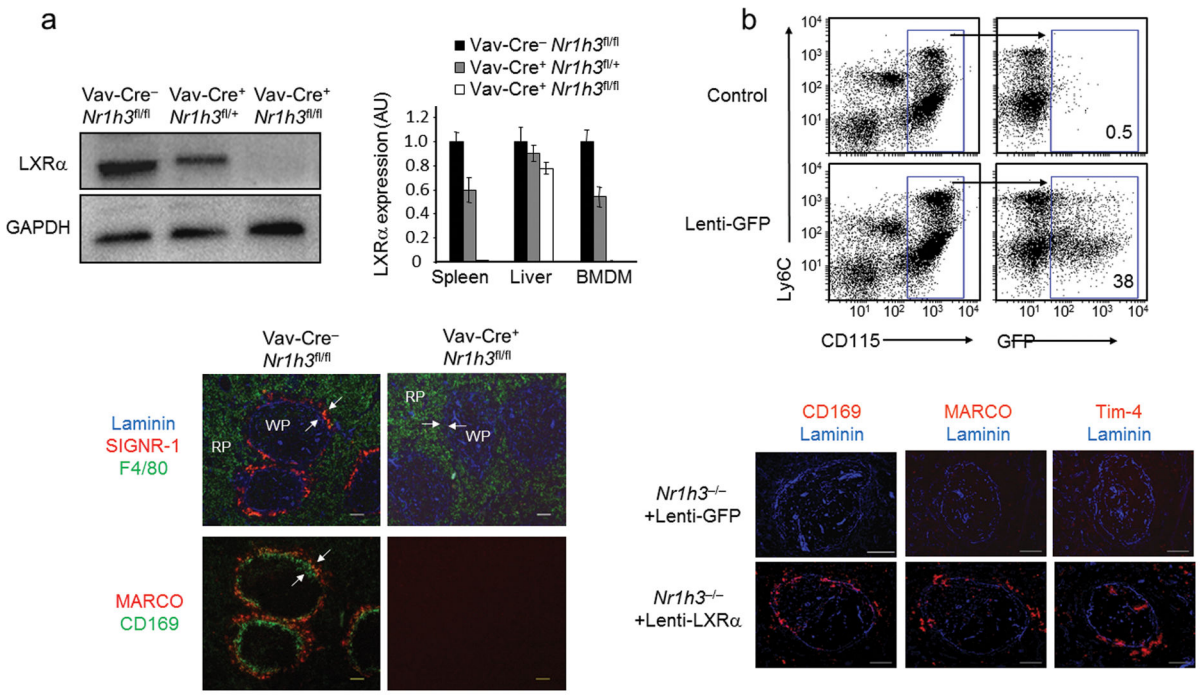

Fig. 6. LXRα function in myeloid cells is required for MZ macrophage development

(a) Immunoblot analysis of LXRα and GADPH in peritoneal macrophages from Vav-Cre^{-}*Nr1h3*$^{fl/fl}$, Vav-Cre^{+}*Nr1h3*$^{fl/+}$, and Vav-Cre^{+}*Nr1h3*$^{fl/fl}$ mice. Right, relative mRNA abundunce of LXRα in spleen, liver and bone marrow derived macrophages (BMDM) from Vav-Cre^{-}*Nr1h3*$^{fl/fl}$, Vav-Cre^{+}*Nr1h3*$^{fl/+}$, and Vav-Cre^{+}*Nr1h3*$^{fl/fl}$ mice. Data are normalized to 36B4 mRNA expression. Data represent mean +/− SEM (n= 2–3 mice). Data are representative of four independent experiments. Immunofluorescence analysis of consecutive sections obtained from Vav-Cre^{-}/*Nr1h3*$^{fl/fl}$ and Vav-Cre^{+}/*Nr1h3*$^{fl/fl}$ spleens that were stained with Laminin, SIGN-R1 and F4/80 antibodies (top); bottom, MZ macrophages (MARCO, red), and marginal metallophilic macrophages (CD169, green); scale bar represents 50 μm. Representative images obtained from four independent experiments with *n* = 3–6 mice per group **(b)** Gain-of-function studies with a macrophage specific lentivirus expressing LXRα. Top, flow cytometry analysis of blood monocytes from WT mice transplanted with HSCs transduced with Lenti-GFP viral particles. Middle, immunofluorescence analysis of macrophage markers in spleen sections from LXRα-KO mice that were transplanted with LXRα-KO HSCs transduced with Lenti-GFP or Lenti-LXRα particles (representative images from two independent experiments with *n* = 4–5 mice per group); scale bar represents 100 μm.

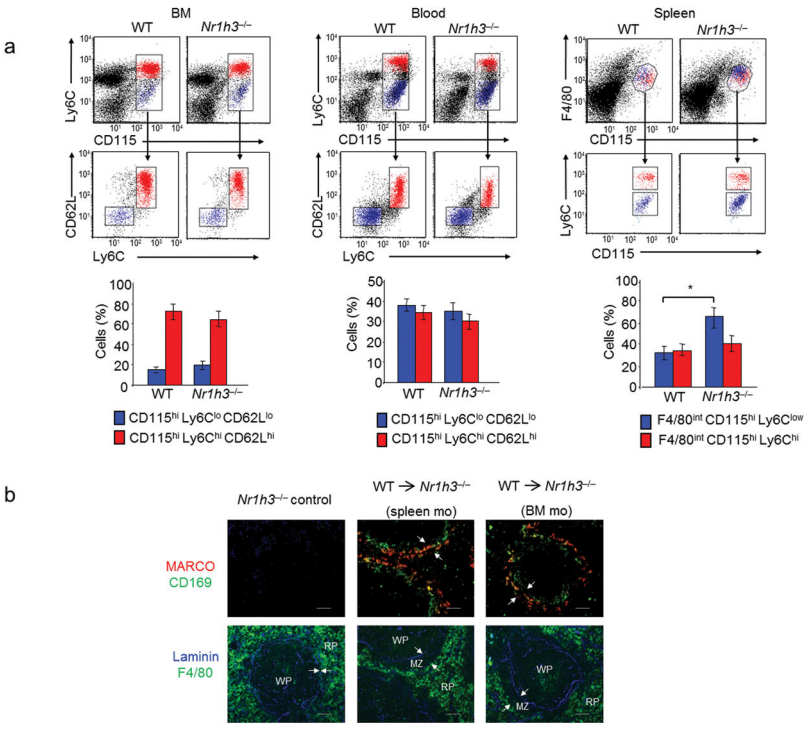

Fig. 7. Adoptive transfer of monocytes reconstitute splenic MZ microenvironment in LXRα-KO mice

(a) Flow cytometry analysis of monocyte subsets in BM, blood and spleen cells from WT and LXRα-KO mice. Classical and non-classical monocytes were detected based on the expression of Ly6C and CD62L in $CD115^+$ cells in BM and blood, and based on the expression of Ly6C in $CD115^+$ $F4/80^+$ cells in spleen. Bottom, percentages of classical and non-classical monocytes in bone marrow, blood and spleen measured by flow cytometry. Bars indicate mean +/− (SEM) from $n = 7$ mice. Data are representative from four independent experiments. **(b)** Immunofluorescence analysis of consecutive spleen sections from non-irradiated LXRα-KO mice reconstituted with the indicated WT monocytes from BM or spleen origin. Arrows indicate the RP and WP borders. Representative images from three independent experiments with $n = 5–6$ mice/group are presented. Scale bar represents 50 μm..

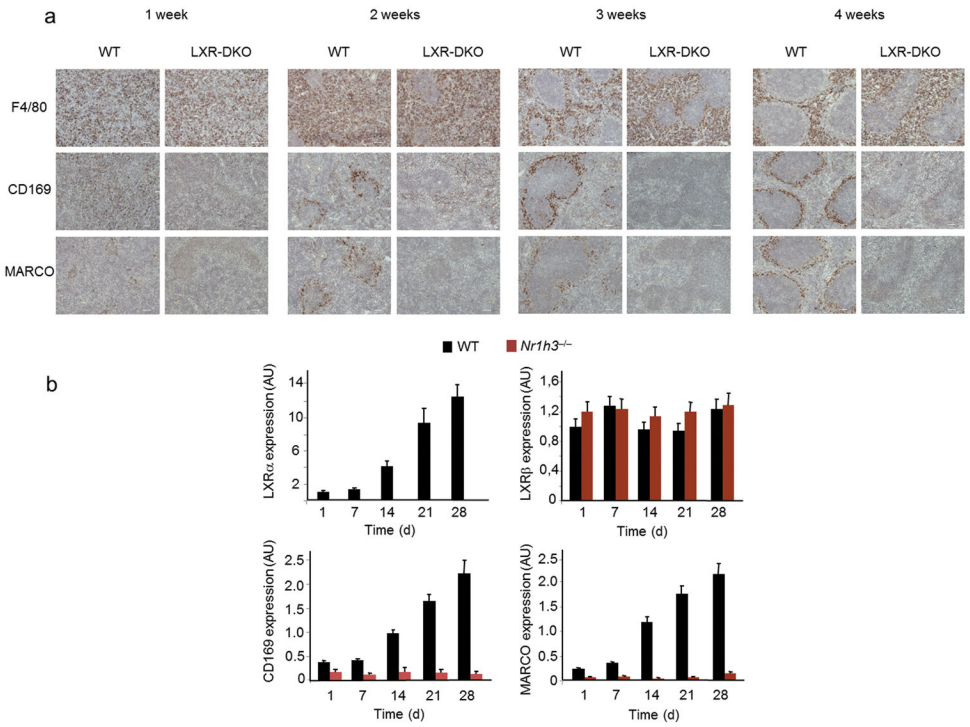

Fig. 8. LXR signaling is necessary for postnatal development of splenic MZ macrophages

a) Immunohistochemical analysis of marginal metallophilic macrophages (CD169), MZ macrophages (MARCO), and red pulp macrophages (F4/80) in spleen sections obtained from WT and LXR-DKO at the indicated times after birth; representative images from three independent experiments with n= 3–4 mice per genotype are presented; scale bar represents 50 μm. **(b)** mRNA relative expression of LXRα, LXRβ, CD169, MARCO, in WT and LXRα-KO spleens at the indicated times after birth. Data represents mean +/− (SEM) obtained from 2 independent experiments with *n* = 6 mice per genotype. Data are normalized to 36B4 mRNA expression.

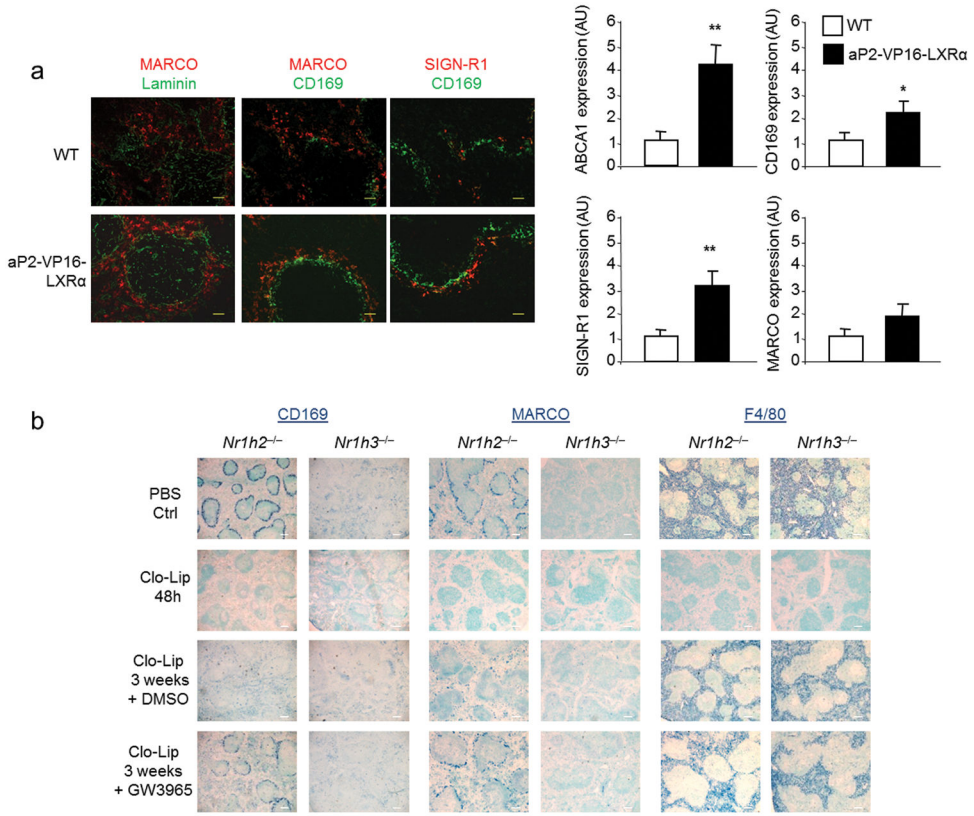

Fig. 9. Activation of LXRα accelerates the development and renewal of MZ macrophages

(a) Immunofluorescence analysis of spleen sections from WT and aP2-VP16-LXRα mice at three weeks of age stained with MARCO, SIGN-R1 (MZ macrophages), CD169 (marginal metallophilic macrophages) and Laminin (endothelial cells) antibodies (left); scale bar represents 25 μm. Right, relative mRNA abundance of ABCA1, CD169, SIGN-R1 and MARCO from spleen samples (*n* = 5) of WT and AP2-VP16-*Nr1h3* spleen at three weeks of age. Data obtained from two independent experiments with n = 3–5 mice **(b)** Immunohistochemistry analysis of CD169, MARCO and F4/80 expression in spleen sections from LXRβ-KO and LXRα-KO mice after clodronate liposome macrophage depletion and GW3965 or vehicle control treatment at the indicated times; scale bar represents 150 μm. Representative images from 2 independent experiments with n = 5–6 mice per group are presented.